华北理工大学
NORTH CHINA UNIVERSITY OF SCIENCE AND TECHNOLOGY

申请专业学位研究生校内指导教师佐证材料

申请人姓名：刘超

专业学位类别：临床医学

专业学位领域：内科学

工作单位：保定市第二医院

2025 年 5 月

目　录

中华人民共和国
居民身份证
签发机关 保定市公安局新市分局
有效期限 2011.03.14-2031.03.14

姓名 刘磊
性别 男
出生 1983 年 6 月 3 日
住址
公民身份号码

普通高等学校

毕业证书

学生 刘超 性别男，一九八三 年 六 月 三日生，于 二〇〇一 年 九 月至二〇〇六年 七 月在本校 临床医学 专业 五 年制本科学习，修完教学计划规定的全部课程，成绩合格，准予毕业。

校 名：河北医科大学 校（院）长：

证书编号：100891200605001584 二〇〇六 年 七 月 一 日

硕士学位证书

刘超，男，1983年6月3日生。在河北联合大学公共卫生与预防医学学科（专业）已通过硕士学位的课程考试和论文答辩，成绩合格。根据《中华人民共和国学位条例》的规定，授予医学硕士学位。

校长

河北联合大学

学位评定委员会主席 袁聚祥

证书编号：T10081320140002O3

二〇一四年六月三十日

河北省专业技术职务任职资格证书

姓　　名（Name）：刘超

性　　别（Gender）：男性

证件类型（Certification Type）：居民身份证（户口簿）

证件号码（Certification No.）：130603198306030016

系　　列（Category）：卫生系列-内科

专　　业（Specialties）：消化内科

资格名称（Title of Qualification）：主任医师（省市级）

批 文 号（Approval No.）：冀职改办字（2022）126号

授予时间（Date of Conferment）：2022年12月28日

工作单位（Place of Work）：保定市第二医院

管 理 号（File No.）：2022A002055

颁证机关：

河北省职称改革领导小组办公室

证书可通过“河北省专业技术职称申报评审信息系统”
网址：http://111.63.208.196:8080 查询核验

保定市科学技术局文件

保科发〔2020〕16号　　签发人：刘铁英

保定市科学技术局
关于下达2020年保定市科技计划自筹经费项目（第一批）的通知

有关县（市、区）科技局，有关单位：

现将2020年保定市科技计划自筹经费项目（第一批）下达给你们，请于8月15日前组织项目承担单位与市科技局签订项目任务书，尽快落实研究任务，并按照《保定市科技计划自筹经费项目管理办法》（保科发〔2020〕15号）的有关规定，加强对项目的组织与管理，确保计划项目的顺利实施。

附件：2020年保定市科技计划自筹经费项目表（第一批）

保定市科学技术局

2020年7月29日

13	2041ZF005	外周血评估PD -1阻断治疗黑色素瘤患者临床疗效价值	安国市医院		2020.06-2021.07	安国市
14	2041ZF006	葛根素促进骨关节炎软骨细胞增殖和减轻氧化应激与炎性反应的机制研究	安国市中医院		2020.02-2021.12	安国市
15	2041ZF007	医学3DV（三维可视化）技术在肝脏外科精准手术中的应用研究	保定市第二医院		2020.04-2022.04	保定市第二医院
16	2041ZF008	加速康复外科(ERAS)联合品管圈（QCC）在肝胆外科围手术期的应用研究	保定市第二医院		2020.04-2022.12	保定市第二医院
17	2041ZF009	冠心病合并2型糖尿病者血浆纤维蛋白原、脂蛋白a、D-二聚体危险因素研究	保定市第二医院		2020.05-2022.03	保定市第二医院
18	2041ZF010	超声联合血清相关因子CRP、TNF-α检测在急性阑尾炎诊断中的应用价值	保定市第二医院		2020.02-2021.06	保定市第二医院
19	2041ZF011	STAT3在宫颈上皮内病变和宫颈癌中的表达及其与高危型HPV感染的关系	保定市第二医院		2020.05-2022.12	保定市第二医院
20	2041ZF012	联合心率变异分析和超声心动图对高龄孕妇的临床研究	保定市第二医院		2020.05-2022.05	保定市第二医院
21	2041ZF013	荞麦多糖对STZ诱导的糖尿病大鼠早期肾损伤的保护作用及降压活性研究	保定市第二医院	首都医科大学三博脑科医院	2020.05-2021.06	保定市第二医院
22	2041ZF014	Lgr5、USP22、Ki67及RASGRAF1基因与结肠癌临床病理特征及预后相关性研究	保定市第二医院		2020.05-2022.05	保定市第二医院
23	2041ZF015	近端和远端胃癌生物学行为差异的分子机制研究	保定市第二医院		2020.05-2022.05	保定市第二医院
24	2041ZF016	不弃血式开放性有创动脉导管采集动脉血气标本的方法研究	保定市第二医院		2020.01-2023.01	保定市第二医院
25	2041ZF017	miR-16通过抑制ERK/MAPK信号通路并影响胶质瘤细胞EMT和侵袭的实验研究	保定市第二医院	首医大三博脑科医院	2020.06-2022.06	保定市第二医院
26	2041ZF018	达格列净联合二甲双胍治疗肥胖/超重2型糖尿病的疗效观察	保定市第二医院		2020.06-2021.12	保定市第二医院
27	2041ZF019	辅助用药在骨科合理应用的研究分析	保定市第二医院		2020.05-2023.05	保定市第二医院
28	2041ZF020	丹参注射液联合复合乳酸菌胶囊治疗溃疡性结肠炎的疗效评估	保定市第二医院		2020.06-2022.06	保定市第二医院
29	2041ZF021	ARID1A、PIK3CA和Ki-67在膀胱尿路上皮癌中的表达及临床病理意义	保定市第二医院		2020.05-2023.05	保定市第二医院
30	2041ZF022	影响突发性耳聋临床疗效相关因素分析	保定市第二医院	保定市儿童医院	2020.01-2022.05	保定市第二医院
31	2041ZF023	不同联合用药方案治疗椎体骨质疏松性骨折的有效性及安全性评价	保定市第二中心医院		2020.06-2022.12	保定市第二中心医院
32	2041ZF024	半枝莲总黄酮调控MIIP对胃癌细胞AGS增殖、凋亡和放疗敏感性影响的研究	保定市第二中心医院		2020.02-2022.02	保定市第二中心医院
33	2041ZF025	脑小血管病变与认知功能障碍及血清炎性因子的相关性研究	保定市第二中心医院		2020.07-2022.07	保定市第二中心医院

保定市社发类项目申请书

(医疗卫生)

社 发 类 别： 消化科

项 目 名 称： 丹参注射液联合复合乳酸菌胶囊治疗溃疡性结肠炎的疗效评估

项目依托单位： 保定市第二医院

参 加 单 位：

项 目 组 长： 刘超

申请资助方式： 完全自筹式

申报项目类别： 应用

项目主管单位： 保定市第二医院

申请计划年度： 2020年

项目起止年月： 2020.06-2022.06

申 报 日 期： 2020-05-27

保定市科学技术局制

<table>
<tr><td rowspan="9">项目依托单位概况</td><td>名称</td><td colspan="5">丹参注射液联合复合乳酸菌胶囊治疗溃疡性结肠炎的疗效评估</td></tr>
<tr><td>地址</td><td colspan="5">保定市东风西路338号</td></tr>
<tr><td>法人代码</td><td colspan="2">40188830-3</td><td>E-mail</td><td colspan="2"></td></tr>
<tr><td>法人代表</td><td>葛长青</td><td>电话</td><td></td><td>邮编</td><td>071051</td></tr>
<tr><td>开户名称</td><td colspan="2">保定市第二医院</td><td>开户银行</td><td colspan="2">保定银行向阳支行</td></tr>
<tr><td>开户行行号</td><td colspan="2">313134000038</td><td>银行账号</td><td colspan="2">86007020105011074</td></tr>
<tr><td>员工总数</td><td>1400 人</td><td>技术人员数</td><td>人</td><td>中高级技术人员数</td><td>人</td></tr>
<tr><td colspan="2">性质</td><td colspan="2">规模</td><td colspan="2">其他特征</td></tr>
<tr><td colspan="2">医院</td><td colspan="2">其他</td><td colspan="2"></td></tr>
<tr><td>项目内容摘要</td><td colspan="5">研究目的：为了评估丹参注射液联合复合乳酸菌胶囊治疗活动期溃疡性结肠炎（UC）的疗效。
方法：将本院收治的64例溃疡性结肠炎患者随机分为对照组与治疗组，每组32例。对照组口服美沙拉嗪肠溶片 4.0g/d，分四次；复合乳酸菌胶囊2粒（0.66g）日三次 口服。治疗组在对照组基础上给予丹参注射液 20ml，加入5%葡萄糖液250ml中，每日一次静滴，观察4周后疗效。
预期结果：经过2周治疗后，对照组排便次数情况与治疗组无明显差异；经过4周治疗后，对照组排便次数情况与治疗组有明显差异。便血量经过2周及4周治疗后，治疗组情况均优于对照组。两组Mayo评分治疗前后有统计学差异。两组血沉（ESR）情况治疗前后有统计学差异。血清血小板（PLT）水平治疗2周后无明显差异，治疗4周后有统计学差异。治疗组与对照组不良反应发生率及对肝肾功能影响情况，均无统计学差异。
预期结论：丹参注射液及复合乳酸菌胶囊联合作用于溃疡性结肠炎治疗效果明显，且费用较低，有长期应用价值，值得推广。</td></tr>
</table>

七、参加人员及分工

序号	姓名	性别	年龄	证件号码	职称	学历	学位	现从事专业	所学专业	所在单位	承担任务（分工）	工作时间
1	刘超	男	36	130603198306030016	副主任医师	本科	硕士	胃肠病学	胃肠病学	保定市第二医院	项目负责人	12
2	杨静	女	36	131022198403040328	主治医师	研究生	硕士	普通外科学	普通外科学	保定市第二医院	资料整理分析	12
3	朱凤池	男	36	130604198410291511	主治医师	研究生	硕士	普通外科学	普通外科学	保定市第二医院	收集整理资料	12
4	乔荼	女	40	13018119800314822X	主治医师	研究生	硕士	胃肠病学	胃肠病学	保定市第二医院	收集整理资料	12
5	马靖	女	38	130602198205101528	主治医师	本科	学士	儿科学	儿科学	保定市第二医院	资料统计	12
6	苏静伟	男	37	130634198308162316	主治医师	本科	学士	普通外科学	普通外科学	曲阳县人民医院	资料统计	12

保定市市级科技计划项目申报诚信承诺书

（申报单位部分）

本单位依据市级科技计划项目指南的任务需求，严格履行法人负责制，自愿提交申报书，**在此郑重承诺：**本单位已就所申报材料内容的真实性和完整性进行审核，不存在违背《关于加强科研诚信建设的实施意见》（冀办字〔2019〕1号）和其它科研诚信要求的行为；申报材料符合《中华人民共和国保守国家秘密法》和《科学技术保密规定》等相关法律法规，在参与项目申报和评审活动全过程中，遵守有关评审规则和工作纪律，杜绝以下行为：

（一）组织或协助、包庇、纵容项目团队以不正当方式影响项目评审公正，获取市级科技计划项目承担资格；

（二）在申报书中以高指标通过评审，在任务书签订时故意篡改降低任务书中相应指标；

（三）其它违反财经纪律和相关管理规定的行为。

如有违反，**本单位愿接受**项目管理机构和相关部门做出的各项处理决定，包括但不限于停拨或核减经费，追回项目经费，取消一定期限市级科技计划项目申报资格，记入科研诚信严重失信行为数据库以及主要负责人接受相应党纪政纪处理等。

申报单位签章：

日期：

保定市市级科技计划项目申报诚信承诺书

（申请人部分）

本人根据市级科技计划项目申报指南的要求自愿提交项目申报书，**在此郑重承诺：**严格落实《关于加强科研诚信建设的实施意见》（冀办字〔2019〕1号）有关要求，所申报材料和相关内容真实有效，不存在违背科研诚信要求的行为；申报材料符合《中华人民共和国保守国家秘密法》和《科学技术保密规定》等相关法律法规；在参与市级科技计划项目申报、评审和实施全过程中，恪守职业规范和科学道德，遵守评审规则和工作纪律，杜绝以下行为：

（一）采取贿赂或变相贿赂、造假、故意重复申报等不正当手段获取科技计划项目承担资格；

（二）抄袭、剽窃他人科研成果或者伪造、篡改研究数据、研究结论；

（三）购买、代写、代投论文，虚构同行评议专家及评议意见；

（四）违反论文署名规范，擅自标注或虚假标注获得科技计划等资助；

（五）在申报书中以高指标通过评审，在任务书签订时故意篡改降低任务书中相应指标；

（六）违反市级科技计划项目管理要求，不按规定提交项目过程管理和验收资料、办理项目结题验收手续；遇不可抗力导致项目无法执行时，不按要求履行项目变更、中止和撤销手续等。

（七）其它违反财经纪律和相关管理规定的行为。

如有违反，本人愿接受项目管理机构和相关部门做出的各项处理决定，包括但不限于取消项目承担资格，追回项目经费，在一定范围内通报违规情况，取消一定期限市级科技计划项目申报资格，记入科研诚信严重失信行为数据库以及接受相应的党纪政纪处理等。

签字：

日期：2020-5-27

九、项目依托单位意见

年　月　日　（公章）

十、项目主管单位意见

年　月　日　（计划专用章）

十一、市科技局意见

年　月　日　（计划专用章）

备注	

保定市科技计划项目任务书

项　目　名　称：丹参注射液联合复合乳酸菌胶囊治疗溃疡性结肠炎的疗效评估

项　目　编　号：2041ZF020

签　订　年　度：2020　　年

项目起止年月：2020.06-2022.06

承担单位（乙方）：保定市第二医院

合　作　单　位：

项　目　负　责　人：刘超　　联系电话：17733221711

开　户　名　称：保定市第二医院

开　户　银　行：保定银行向阳支行

开户银行行号：313134000038

账　　号：86007020105011074

归口管理部门（丙方）：保定市第二医院

保定市科学技术局制

五、参加人员及分工

序号	姓名	性别	年龄	证件号码	职称	学历	学位	现从事专业	单位名称	分工
1	刘超	男	36	130603198306030016	副主任医师	本科	硕士	胃肠病学	保定市第二医院	项目负责人
2	杨静	女	36	131022198403040328	主治医师	研究生	硕士	普通外科学	保定市第二医院	资料整理分析
3	朱凤池	男	36	130604198410291511	主治医师	研究生	硕士	普通外科学	保定市第二医院	收集整理资料
4	乔荼	女	40	13018119800314822X	主治医师	研究生	硕士	胃肠病学	保定市第二医院	收集整理资料
5	马靖	女	38	130602198205101528	主治医师	本科	学士	儿科学	保定市第二医院	资料统计
6	苏静伟	男	37	130634198308162316	主治医师	本科	学士	普通外科学	曲阳县人民医院	资料统计

八、承诺条款

签约各方共遵守市科技计划管理有关规定前提下，承诺如下；

乙方：

1、保证项目实施所必需的场所、仪器、设备等支撑条件。

2、严格按照国家、省和市有关规定及本任务书要求使用科技局拨款。

3、按任务书要求完成市科技局下达的计划任务，接受科技局及其授权或委托机构的监督和评估。

4、项目实行验收结题制，项目验收后向甲方、乙方填报验收证书。

丙方：

1、协助甲方组织和实施项目，监督和检验乙方对任务书的执行。

2、负责初审任务书内容，向甲方报告项目进展情况和经费决算。

3、受甲方委托组织项目的验收工作。

甲方：

1、 定期对项目进度监督检验和验收，协调解决项目进行中出现的问题。

2、 按任务书规定的用款计划拨给乙方当年的科研经费。

3、 对于不能恰当履行任务书义务的乙方、丙方，应通报批评，并视情况终止或撤消项目。此款将作为对承担单位和项目负责人信誉评估的重要依据。

本任务书所协议的其它条款如下

九、 任务书签订各方签章

甲方：保定市科学技术局

（计划专用章）

主管业务处处长：

日期：

主管局长：

日期：

乙方（承担单位）：保定市第二医院

（公章）

项目负责人：

日期：

所在单位负责人：

日期：

合作单位：

（公章）

日期：

丙方（归口管理单位）：保定市第二医院

（科研计划专用章）

负　　责　　人：

日期：

经　　办　　人：

日期：

保定市科技计划项目验收证书

保科验字（2021）03-157 号

项 目 编 号：2041ZF020

项 目 名 称：丹参注射液联合复合乳酸菌胶囊治疗溃疡性结肠炎的疗效评估

承 担 单 位：保定市第二医院

合 作 单 位：

验收主持部门：市科技局

验 收 方 式：函审验收

验 收 日 期：2021-09-03

保定市科学技术局制

一、项目基本信息

<table>
<tr><td>项目名称</td><td colspan="8">丹参注射液联合复合乳酸菌胶囊治疗溃疡性结肠炎的疗效评估</td></tr>
<tr><td>第一承担单位名称</td><td colspan="3">保定市第二医院</td><td>单位性质</td><td colspan="4">医院</td></tr>
<tr><td rowspan="2">项目负责人</td><td>姓名</td><td>刘超</td><td>联系电话</td><td>0312-3099725</td><td>电子邮箱</td><td colspan="3">liuchao1936@163.com</td></tr>
<tr><td>学历</td><td>本科</td><td>学位</td><td>硕士</td><td>职称</td><td colspan="3">副主任医师</td></tr>
<tr><td rowspan="3">参研人员情况</td><td rowspan="2">总人数（人）</td><td colspan="4">按专业技术职务分布</td><td colspan="4">按学位分布</td></tr>
<tr><td>高级职称</td><td>中级职称</td><td>初级职称</td><td>其它人员</td><td>博士</td><td>硕士</td><td>学士</td><td>其它</td></tr>
<tr><td>6</td><td>1</td><td>5</td><td>0</td><td>0</td><td>0</td><td>4</td><td>1</td><td>1</td></tr>
<tr><td colspan="5">累计投入项目研究的工作量（人月）</td><td>6</td><td colspan="2">吸引省外人才（人）</td><td>0</td></tr>
<tr><td>所属领域</td><td colspan="8">医疗卫生技术</td></tr>
<tr><td rowspan="2">产学研联合</td><td>主要合作单位名称</td><td colspan="3"></td><td>合作单位性质</td><td colspan="3"></td></tr>
<tr><td>合作形式</td><td colspan="7"></td></tr>
<tr><td rowspan="2">累计经费筹集情况（万元）</td><td>总投入</td><td>省科技厅拨款</td><td>市科技局拨款</td><td>市县匹配资金</td><td>单位自筹</td><td>银行贷款</td><td colspan="2">其他</td></tr>
<tr><td>3.8</td><td>0</td><td>0</td><td>0</td><td>3.8</td><td>0</td><td colspan="2">0</td></tr>
<tr><td rowspan="2">累计实现的直接经济效益</td><td colspan="2">新增产值（万元）</td><td>0</td><td colspan="3">出口创汇（万美元）</td><td colspan="2">0</td></tr>
<tr><td colspan="2">上缴税金（万元）</td><td>0</td><td colspan="3">净利润额（万元）</td><td colspan="2">0</td></tr>
</table>

<table>
<tr><td rowspan="13">累计实现的直接社会效益</td><td>成果转让数（项）</td><td>0</td><td>成果转让获得收入（万元）</td><td>0</td><td>获省部级以上奖励（项）</td><td>0</td></tr>
<tr><td>新产品、新材料（种）</td><td>0</td><td>新工艺、新装置（项）</td><td>0</td><td>出版科技著作（万字）</td><td>0</td></tr>
<tr><td>科技论文、报告（篇）</td><td>8</td><td>其中：发表科技论文（篇）</td><td>8</td><td>其中：被EI、SCI、ISTP、ISR收录（篇）</td><td>0</td></tr>
<tr><td colspan="2">动植物新品种开发个数（个）</td><td>0</td><td colspan="2">动植物新品种推广面积或扩繁数量（亩或头）</td><td>0</td></tr>
<tr><td colspan="2">累计建立试验示范区（基地）数（个）</td><td>0</td><td colspan="2">累计建立试验示范区规模（亩或头）</td><td>0</td></tr>
<tr><td colspan="2">专利申请数（项）</td><td>发明</td><td>实用新型</td><td>外观设计</td><td></td></tr>
<tr><td colspan="2">0</td><td>0</td><td>0</td><td>0</td><td></td></tr>
<tr><td colspan="2">专利授权数（项）</td><td>发明</td><td>实用新型</td><td>外观设计</td><td></td></tr>
<tr><td colspan="2">0</td><td>0</td><td>0</td><td>0</td><td></td></tr>
<tr><td colspan="2">制定技术标准（项）</td><td>企业标准</td><td>地方标准</td><td>行业标准</td><td>国家标准</td><td>国际标准</td></tr>
<tr><td colspan="2">0</td><td>0</td><td>0</td><td>0</td><td>0</td><td>0</td></tr>
<tr><td colspan="2">培养人才数（人）</td><td colspan="2">获博士学位人数</td><td colspan="2">获硕士学位人数</td><td>培训专业技术人员（人次）</td></tr>
<tr><td colspan="2">0</td><td colspan="2">0</td><td colspan="2">0</td><td>0</td></tr>
<tr><td rowspan="2">累计环保节能效益</td><td>节 煤（万吨）</td><td>0</td><td>节电（万度）</td><td>0</td><td>节 水（万吨）</td><td>0</td></tr>
<tr><td>减排废气（万立方米）</td><td>0</td><td>减排废水（万吨）</td><td>0</td><td>减排废物（万吨）</td><td>0</td></tr>
</table>

注：1、本表由完成单位如实填写，无填报内容可空缺；

2、累计情况请填报自项目开始实施至结题的合计数；

3、本表数据做为项目绩效评价的参考依据。

四、主要研制人员名单

序号	姓名	性别	年龄	职称	学历	学位	现从事专业	单位名称	分工	本人签名
1	刘超	男	36	副主任医师	本科	硕士	胃肠病学	保定市第二医院	项目负责人	
2	杨静	女	36	主治医师	研究生	硕士	普通外科学	保定市第二医院	资料整理分析	
3	朱凤池	男	36	主治医师	研究生	硕士	普通外科学	保定市第二医院	收集整理资料	
4	乔荼	女	40	主治医师	研究生	硕士	胃肠病学	保定市第二医院	收集整理资料	
5	赵丹阳	女	32	其他中级	本科	无	胃肠病学	保定市人民医院	资料统计	
6	苏静伟	男	37	主治医师	本科	学士	普通外科学	曲阳县人民医院	资料统计	

四、验收专家名单

序号	姓　名	工 作 单 位	所学专业	现从事学科	职务/职称	本人签名
1	赵东强	河北医科大学第二附属医院	胃肠病学	胃肠病学	主任医师	赵东强
2	杨川杰	河北医科大学第二附属医院	胃肠病学	胃肠病学	主任医师	杨川杰
3	王丽璞	保定市第一中医院	中医外科学	中医外科学	主任医师	
4	郝福庆	河北大学附属医院	内科其他学科	全科医学	主任医师	
5	廖振林	保定市第一医院	胃肠病学	胃肠病学	主任医师	廖振林

六、验收意见

由保定市第二医院承担的保定市科学技术研究与发展指导计划项目“丹参注射液联合复合乳酸菌胶囊治疗溃疡性结肠炎的疗效评估”（编号2041ZF020），已按项目申报书或任务书完成，经审查，提供的技术资料完整、规范，符合验收要求。综合其他委员意见，形成验收意见如下：

通过本研究评估丹参注射液联合复合乳酸菌胶囊治疗溃疡性结肠炎的疗效，得出结论溃疡性结肠炎患者通过给与丹参注射液联合复合乳酸菌胶囊的治疗方案，可明显改善患者的临床症状，缩短治疗时间，减少住院费用，具有较好的社会效益。

综上所述，承担单位完成了项目申报书或任务书规定的各项指标，具有显著的社会效益，推广应用前景广阔，切合临床实际，观察指标全面，为溃疡性结肠炎的治疗提供新的治疗方案，验收组一致同意通过验收。

建议：延长观察时间，扩大研究病例数量，为临床研究提供更多依据。

五、验收意见

由保定市第二医院承担的保定市科学技术研究与发展指导计划项目“丹参注射液联合复合乳酸菌胶囊治疗溃疡性结肠炎的疗效评估”（编号 2041ZF020），已按项目申报书或任务书完成，经审查，提供的技术资料完整、规范，符合验收要求。综合其他委员意见，形成验收意见如下：

通过本研究评估丹参注射液联合复合乳酸菌胶囊治疗溃疡性结肠炎的疗效，得出结论溃疡性结肠炎患者通过给与丹参注射液联合复合乳酸菌胶囊的治疗方案，可明显改善患者的临床症状，缩短治疗时间，减少住院费用，具有较好的社会效益。

综上所述，承担单位完成了项目申报书或任务书规定的各项指标，具有显著的社会效益，推广应用前景广阔，切合临床实际，观察指标全面，为溃疡性结肠炎的治疗提供新的治疗方案，验收组一致同意通过验收。

建议：延长观察时间，扩大研究病例数量，为临床研究提供更多依据。

验收委员会主任：赵东强

_____年_____月_____日

七、项目管理部门意见

项目承担单位意见

负责人签字：　　（公章）

2024年9月14日

项目归口管理部门意见

负责人签字：

（科研管理章）

2024年9月14日

市科技局意见

项目主管处室负责人签字：郝春菊

（科技项目验收专用章）

年　月　日

河北省科学技术成果

证书

河北省科学技术厅

成果名称：丹参注射液联合复合乳酸菌胶囊治疗溃疡性结肠炎的疗效评估

完 成 人：刘　超（第壹完成人）

所在单位：保定市第二医院

第一完成单位：保定市第二医院

省级登记号：20212312

二〇二一年十一月

科技成果登记专用章

证 书

编　号：212597-1

为表彰荣获河北医学科技奖的优秀医学科技工作者，特发此证，以资鼓励。

成果名称：丹参注射液联合复合乳酸菌胶囊治疗溃疡性结肠炎的疗效评估

完成单位：保定市第二医院
保定市人民医院

完 成 人：刘 超　杨 静　朱凤池　乔 茶　赵丹阳

奖励等级：贰等奖

河北省医学会

2022年4月

附表 1

应用证明

项目名称	丹参注射液联合复合乳酸菌胶囊治疗溃疡性结肠炎的疗效评估	
应用单位	保定市第二医院	
单位注册地址	河北省保定市东风西路 338 号	
应用起止时间	2020 年 06 月 至 2021 年 07 月	
经济效益（万元）		
自然年	新增销售额	新增利润
2018 年		
2019 年		
2020 年		
累　计		

所列经济效益的有关说明及计算依据：

应用单位财务章

年　月　日

具体应用情况：

溃疡性结肠炎(UC)是一种发病率较高的疾病，易反复发作、病程迁延，治愈难度大。丹参注射液具有疏通微循环，降低血液黏滞度的作用。复合乳酸菌胶囊含有乳酸杆菌、嗜乳酸杆菌和乳酸链球菌三种活乳酸菌。本研究创新性的应用丹参注射液及复合乳酸菌胶囊联合作用于溃疡性结肠炎治疗效果明显，改善患者的生活质量及预后，提高患者的满意率，且费用较低，具有较好的经济效益和社会效益。

应用单位法定代表人签名：	
青葛印长 年 月 日	市第二医院 应用单位公章 年 月 日

注：无经济效益的项目，可不填经济效益相关栏目、不加盖应用单位财务章

27

报告编号：L24M2023-0003

检　索　报　告

一、检索要求

1. 委 托 人：刘超(Liu, C (Liu, Chao))
2. 委托单位：保定市第二医院
3. 检索目的：论文被 SCI-E 收录情况

二、检索范围

Science Citation Index Expanded (SCI-EXPANDED)	1990-present	网络版
JCR-(Journal Citation Reports)	2021	网络版

三、检索结果

委托人提供的1篇论文被SCI-E收录，论文收录及其所在期刊的JCR影响因子、JCR分区情况见附件一。

特此证明！

检索报告人：谢福秀

东北师范大学科技查新咨询中心

教育部科技查新工作站(L24)

2023 年 1 月 3 日

附件一：SCI-E收录情况

1 record(s) printed from Clarivate Web of Science

第 1 条，共 1 条

标题: Exosomal circ_0001190 Regulates the Progression of Gastric Cancer via miR-586/SOSTDC1 Axis

作者: Liu, C (Liu, Chao); Yang, J (Yang, Jing); Zhu, FC (Zhu, Fengchi); Zhao, ZY (Zhao, Zhiying); Gao, LX (Gao, Lixue)

来源出版物: BIOCHEMICAL GENETICS **卷:** 60 **期:** 6 **页:** 1895-1913 **DOI:** 10.1007/s10528-021-10180-6 **提前访问日期:** FEB 2022 **出版年:** DEC 2022

Web of Science 核心合集中的 "被引频次": 2

被引频次合计: 2

使用次数 (最近 180 天): 0

使用次数 (2013 年至今): 1

引用的参考文献数: 42

摘要: Gastric cancer (GC) is the fifth most common cancer, which has a significant impact on human health. Recent researches have shown that circular RNAs (circRNAs) could affect the progress of GC, but the mechanism still indistinct. In this work, we explored the roles of circ_0001190 in GC. The levels of circ_0001190, microRNA-586 (miR-586) and sclerostin domain containing 1 (SOSTDC1) were detected by quantitative RT-PCR and western blot in GC. The cell functions were scrutinized by cell counting kit-8 assay, 5-Ethynyl-29-deoxyuridine assay, flow cytometry assay, tube formation assay, transwell assay, and western blot. Furthermore, the relationship between miR-586 and circ_0001190 or SOSTDC1 was identified by dual-luciferase reporter assay. Finally, the xenograft model test was implemented to demonstrate the effect of exosomal circ_0001190 in vivo. The levels of circ_0001190 and SOSTDC1 were downregulated, and the miR-586 level was increased in GC. For functional assay, circ _0001190 overexpression inhibited cell vitality, cell proliferation, angiogenesis, cell migration and invasion, whereas stimulated cell apoptosis in GC cells. Circ _0001190 served as a miR-586 sponge to adjust the expression of SOSTDC1. Additionally, miR-586 could promote the advancement of GC by interfering SOSTDC1. Exosomal circ_0001190 overexpression inhibited the development of GC by miR-586/SOSTDC1 axis, which proposed a potential targeted therapy for GC cure.

入藏号: WOS:000753226600002

PubMed ID: 35138469

语言: English

文献类型: Article

作者关键词: Gastric cancer; Exosomal circ_0001190; miR-586; SOSTDC1

KeyWords Plus: CELL-PROLIFERATION; SOSTDC1; EXPRESSION; ANTAGONIST; MICRORNAS; MIGRATION; INVASION; MARKER

地址: [Liu, Chao; Zhao, Zhiying] 2 Hosp Baoding, Dept Gastroenterol, Baoding City 071051, Hebei, Peoples R China.
[Yang, Jing; Zhu, Fengchi] 2 Hosp Baoding, Dept Anorectal Surg, Baoding City 071051, Hebei, Peoples R China.
[Gao, Lixue] 2 Hosp Baoding, Dept Surg Oncol, 338 Dongfeng West Rd, Baoding City 071051, Hebei, Peoples R China.

通讯作者地址: Gao, LX (通讯作者), 2 Hosp Baoding, Dept Surg Oncol, 338 Dongfeng West Rd, Baoding City 071051, Hebei, Peoples R China.

电子邮件地址: wkysglx@163.com

出版商: SPRINGER/PLENUM PUBLISHERS

出版商地址: 233 SPRING ST, NEW YORK, NY 10013 USA

Web of Science Index: Science Citation Index Expanded (SCI-EXPANDED)

Web of Science 类别: Biochemistry & Molecular Biology; Genetics & Heredity

研究方向: Biochemistry & Molecular Biology; Genetics & Heredity

IDS 号: 5U5OJ
ISSN: 0006-2928
eISSN: 1573-4927
29 字符的来源出版物名称缩写: BIOCHEM GENET
ISO 来源出版物缩写: Biochem. Genet.
来源出版物页码计数: 19
输出日期: 2023-01-03

End of File

INTEGRATIVE CANCER THERAPIES 期刊影响因子 ™ 2021：2.22

期刊 JCR 分区(2021)截图如下：

BIOCHEMICAL GENETICS

期刊影响因子™

2021	五年
2.22	2.077

JCR 学科类别	类别排序	类别分区
BIOCHEMISTRY & MOLECULAR BIOLOGY *其中 SCIE 版本*	256/297	Q4
GENETICS & HEREDITY *其中 SCIE 版本*	133/175	Q4

来源: Journal Citation Reports 2021. 进一步了解

—The End—

Biochemical Genetics
https://doi.org/10.1007/s10528-021-10180-6

ORIGINAL ARTICLE

Exosomal circ_0001190 Regulates the Progression of Gastric Cancer via miR-586/SOSTDC1 Axis

Chao Liu[1] · Jing Yang[2] · Fengchi Zhu[2] · Zhiying Zhao[1] · Lixue Gao[3]

Received: 2 September 2021 / Accepted: 20 December 2021

Abstract

Gastric cancer (GC) is the fifth most common cancer, which has a significant impact on human health. Recent researches have shown that circular RNAs (circRNAs) could affect the progress of GC, but the mechanism still indistinct. In this work, we explored the roles of circ_0001190 in GC. The levels of circ_0001190, microRNA-586 (miR-586) and sclerostin domain containing 1 (SOSTDC1) were detected by quantitative RT-PCR and western blot in GC. The cell functions were scrutinized by cell counting kit-8 assay, 5-Ethynyl-29-deoxyuridine assay, flow cytometry assay, tube formation assay, transwell assay, and western blot. Furthermore, the relationship between miR-586 and circ_0001190 or SOSTDC1 was identified by dual-luciferase reporter assay. Finally, the xenograft model test was implemented to demonstrate the effect of exosomal circ_0001190 in vivo. The levels of circ_0001190 and SOSTDC1 were downregulated, and the miR-586 level was increased in GC. For functional assay, circ _0001190 overexpression inhibited cell vitality, cell proliferation, angiogenesis, cell migration and invasion, whereas stimulated cell apoptosis in GC cells. Circ _0001190 served as a miR-586 sponge to adjust the expression of SOSTDC1. Additionally, miR-586 could promote the advancement of GC by interfering SOSTDC1. Exosomal circ_0001190 overexpression inhibited the development of GC by miR-586/SOSTDC1 axis, which proposed a potential targeted therapy for GC cure.

Keywords Gastric cancer · Exosomal circ_0001190 · miR-586 · SOSTDC1

✉ Lixue Gao
wkysglx@163.com

1 Department of Gastroenterology, the No 2 Hospital of Baoding, Baoding City 071051, Hebei, China

2 Department of Anorectal Surgery, the No 2 Hospital of Baoding, Baoding City 071051, Hebei, China

3 Department of Surgical Oncology, the No 2 Hospital of Baoding, No.338 Dongfeng West Road, Baoding City 071051, Hebei, China

Published online: 09 February 2022

Introduction

Gastric cancer (GC) is a common cancer and its mortality is the second worldwide (Bray et al. 2018; Song et al. 2017). The five-year survival rate of GC is 20%–40% (Allemani et al. 2018). Analysis of the age of onset in recent years showed that the risk was increased in younger people (Lee et al. 2017). Patients with GC have the characteristics of high metastasis rate and mortality, and the effect of current treatment methods is not ideal (Sun et al. 2015). Therefore, we urgently need to find a new way for GC treatment.

Circular RNAs (circRNAs) are a kind of RNAs that have no 5'-caps and 3'-tails, which can stably exist in plentiful types of organisms and play important roles in various cellular processes (Ambros 2004; Garzon et al. 2010). For instance, hsa_circ_0004872 overexpression hindered the invasion and migration of GC cells (Ma et al. 2020). Besides, hsa_circ_006100 stimulated cell growth and metastasis (Liang 2019). In addition, circ_0000190 induced apoptosis and cell cycle arrest in GC (Wang et al. 2020a). Previous studies have shown that circ_0001190 was significantly downregulated in both tumor tissues and plasma of GC patients (Liu et al. 2020; Li et al. 2018). Therefore, we speculated that circ_0001190 was of great significance to the growth of GC. However, the functions of circ_0001190 on GC is ill-defined.

MicroRNAs (miRNAs) are a type of small RNAs, which regulates the subsequent biology processes (Ambros 2004; Garzon et al. 2010). For example, miRNA-586 low expression was a mark of poor prognosis in glioma (Luo et al. 2020). Moreover, miR-21 took part in regulating cisplatin resistance in GC (Zheng et al. 2017). In addition, miR-129-5p inhibited cell proliferation in GC (Wang and Yu 2018). However, the understanding of the influence of miR-586 in GC still restricted.

Previous studies have shown that sclerostin domain containing 1 (SOSTDC1) played an indispensable role in the formation of teeth, hair follicles, and trigeminal ganglion (Ahn et al. 2017; Narhi et al. 2012; Shigetani et al. 2008). In addition, SOSTDC1 was involved in regulating cell differentiation and proliferation (Chen et al. 2018). Moreover, SOSTDC1 inhibited cell migration in follicular thyroid cancer (Zhou et al. 2017). However, the relationship between SOSTDC1 and the GC is still indistinct, which is worth studying in detail.

In this paper, we studied the molecular regulation mechanism of circ_0001190 in GC. The research revealed that circ_0001190 suppressed the progression of GC. Our consequences might provide innovative ideas for targeted therapy of GC and provide molecular theoretical basis for subsequent clinical treatment.

Materials and Methods

Clinical Tissue Samples

The research was approved by the No 2 Hospital of Baoding. Forty pairs of GC tissues were employed to qRT-PCR. In addition, blood samples from 10 GC sufferers and 10 healthy controls (not diagnosed with cancer) were collected for exosome extraction. All samples were gathered from the No 2 Hospital of Baoding. All the volunteers signed informed consent forms. Afterward, all samples were conserved at − 80 °C.

Cell lines and Cell Culture

The human GC cell lines (HGC27, AGS, MKN45, MKN47 and N87), with GES-1 cells as control. Human Umbilical Vein Endothelial Cells (HUVECs) were used for tube formation assay. All cells were bought from Cell Bank, Chinese Academy of Sciences (CAS, Shanghai, China). These cells were cultivated with RPMI 1640 medium (Gibco, Carlsbad, CA, USA) and F12K medium (Gibco, only for AGS) in 5% CO_2.

Exosome Isolation and Identification

Exosomes from cells are collected from cell culture medium or serum. As described by Xie et al., the cell culture medium or serum was centrifuged and the product was washed (Xie et al. 2020). Then ExoQuick Exosome (SBI, CA, USA) precipitated solution was added according to the instructions, refrigerated and centrifuged, and sterile PBS was used to re-suspend exosome particles. Finally, transmission electron microscopy was used to identify the size and form of exosomes. The particle size was detected by Nanoparticle tracking analysis (NTA). Exosome protein markers were assessed by western blot analysis.

Quantitative RT-PCR

RNA was separated by Trizol (Sigma-Aldrich, St. Louis, MO, USA). Whereafter, entire RNA was reverse-transcribed to complementary DNA. The Prime Script RT reagent kit (Thermo Fisher Scientific, Waltham, MA, USA) was applied for circ_0001190 and SOSTDC1 reverse transcription. Meanwhile, miRNA was reverse-transcribed using a miRNA First-Strand Synthesis kit (Takara, Tokyo, Japan) for miR-586. Next, cDNA was applied for qRT-PCR with an SYBR Green kit (Takara). GAPDH and RNU6 (U6) were used as endogenous controls to standardize circRNA and miRNA expression levels, respectively. The primers are listed in Table 1. Relative abundance was computed by the $2^{-\Delta\Delta Ct}$ method.

Table 1 Primers sequences used for PCR

Name	Primers (5′-3′)	
circ_0001190	Forward	TGCAGGAACTATTTCTCAGCATTG
	Reverse	AAGAGTCCAGCGGCAAAACT
SOSTDC1	Forward	CCGTACCCAGAGAATCCAGC
	Reverse	ATTTGCTGGCTCTTTTCCGC
miR-586	Forward	GCCGAGTATGCATTGTATTTTTA
	Reverse	CTCAACTGGTGTCGTGGA
GAPDH	Forward	TCCCATCACCATCTTCCAGG
	Reverse	GATGACCCTTTTGGCTCCC
U6	Forward	CTCGCTTCGGCAGCACATATACT
	Reverse	ACGCTTCACGAATTTGCGTGTC
miR-576-5p	Forward	GCCGAGATTCTAATTTCTCCACG
	Reverse	CTCAACTGGTGTCGTGGA
miR-512-5p	Forward	CGGGCGGCACTCAGCCTTGAGGG
	Reverse	CTCAACTGGTGTCGTGGA
miR-1827	Forward	GGGGTGAGGCAGTAGATTG
	Reverse	CTCAACTGGTGTCGTGGA
miR-568	Forward	GCCGAGATGTATAAATGTATACACA
	Reverse	CTCAACTGGTGTCGTGGA
miR-665	Forward	GGTGAACCAGGAGGCTGAGG
	Reverse	CTCAACTGGTGTCGTGGA
DYRK1A	Forward	GTTCGGGCTCTCCTGGC
	Reverse	CTCAGTCTCTCCTCGGCTCG

Western Blot

The method of western blot was as previously reported (Hou and Zhang 2021). The GC cells were treated with a RIPA buffer (Sigma), and the protein content was assessed through a BCA kit (Sigma). The disconnected protein was moved to a 10% SDS-PAGE and therewith transferred to PVDF membranes (Sigma). Subsequently, the membranes were hatched with the nether primary antibodies: anti-CD9 (ab92726; 1:1000; Abcam, Cambridge, MA, USA), anti-CD63 (ab119992; 1:1000; Abcam), anti-TSG101 (ab125011; 1:1000; Abcam), anti-Ki67 (ab92742; 1:1,000; Abcam), anti-Bax (ab32503; 1:1,000; Abcam), anti-MMP-2 (ab92536; 1:1000; Abcam), anti-SOSTDC1 (SAB2107833; 1:1000; Sigma), and anti-β-actin (ab8226; 1:1000; Abcam). Conclusively, the membranes were hatched with a secondary antibody (ab205718; 1:2500; Abcam) for 1 h. Finally, the protein band was observed.

RNase R Degradation Assay

On the basis of the RNase R kit directions (Sigma), the RNA was treated with RNase R. Moreover, the DYRK1A mRNA was employed as control. The RNA

(5 μL) was disposed of RNase R (10 U, Sigma) for 30 min. At that moment, the levels of circ_0001190 and DYRK1A mRNA were detected.

Cell Transfection

The circ_0001190 exo, the control (vector exo), miR-586 mimic, and miR-NC, the si-SOSTDC1 and control (si-NC) were acquired from Ribobio (Guangzhou, China). These plasmids or oligonucleotides were transferred in into GC cells by utilizing Lipofectamine 2000 (Thermo Fisher Scientific).

CCK8 Assay

After post-transfection, GC cells (2.0×10^3/well) were planted in 96-well plates. Then, the CCK8 (20 μL, Sigma) was supplemented and nurture 4 h. The OD value was assessed at 450 nm to confirm the cell viability.

Cell Proliferation Assay

After transfection, GC cells were seeded into 96-well plates. Then, the EdU Apollo in Vitro Imaging Kit (RiboBio) was used as stated by the guide. GC cells were incubated with EdU and exposed to paraformaldehyde (4%, RiboBio) for 30 min. Following, the Triton X-100 and Apollo solution were added. In the end, cells were exposed to DAPI (RiboBio).

Flow Cytometry Assay

GC cells after varied transfection were planted in 96-well plates. As the described by Wang et al., the Annexin V-FITC Apoptosis Detection Kit (Sigma) was used to treat every group cells (Wang et al. 2020b). The apoptotic cells were observed under a flow cytometry.

Tube Formation Assay

HUVECs (4×10^5 cells/well) with different treatment were planted into Matrigel-coated 96-well plates. Meanwhile, the tube formation rate was examined after 24 h. Afterward, Image J software (NIH, Bethesda, MD, USA) was used to observe the number of tubes and the count of branches. The elongated multi-cellular structures were considered tube-like structures. The intersecting points of two or more tubes were considered branches.

Transwell Assay

After 48 h transfection, GC cells were performed in a transwell with 8 μm pore polycarbonate membrane (Corning, MA, USA). GC cells (4×10^5) were planted on the

upper chambers coated in serum-free medium. Then, 500 μL of DMEM comprising 10% FBS was added to the inferior chamber of the transwell. The same method was used, but transwell chamber precoated Matrigel (Corning) was implemented to evaluate the invasion. After 12 h, cells were fixed and exposed to crystal violet solution, and observed under a light microscope.

Dual-luciferase Reporter Assay

The binding site between miR-586 with circ_0001190 or SOSTDC1 was estimated by circinteractome (https://circinteractome.nia.nih.gov), circbank (http://www.circbank.cn/) and targetscan (http://www.targetscan.org). Then, the wild type and mutant circ_0001190 and SOSTDC1 were manufactured by Ribobio (circ_0001190 WT, SOSTDC1 3'UTR WT or circ_0001190 MUT, SOSTDC1 3'UTR MUT). The luciferase activity was tested.

RNA Pull-Down

The Bio-miR-586, Bio-miR-586 MUT, and control (Bio-NC) were manufactured by RiboBio. A RNA–Protein Pull-Down Kit (Sigma) was utilized to recognize the interaction among circ_0001190 and miR-586. After post-transfection, GC cells were nurtured with the probe-bead compound for 3 h. Next, the beads were collected, and removed the protein and DNA, respectively. Lastly, the level of circ_0001190 was measured.

Xenograft Models

The research was approved by the Animal Care and Use Committee of the No 2 Hospital of Baoding. All nude mice were got from Beijing Vital River Laboratory Animal Technology (Beijing, China). HGC27 cells (1×10^6) with circ_0001190 or the vector exo were inoculated into mice (female, two groups, n = 6/group, 6 weeks, 18–22 g). Lastly, tumor volume was registered once a week suitable for the formula: Tumor volume = length × width^2 × 0.5. After 35 days, the tumor tissues were carved for supplementary experiment.

Immunohistochemistry (IHC) Assay

The IHC was carried out as Qiu et al. described (Qiu et al. 2018). The slice was sealed by peroxidase and exposed to PBS that comprised 10% skim milk about 20 min to seal particular sites. The SOSTDC1 primary antibody (ab99340; 1:1,000; Abcam) and Ki67 (ab16667; 1:1,000; Abcam) were hatched. Next, the secondary antibody (ab150113, Abcam) conjugated with HRP was incubated for 30 min. Eventually, the slides were stained using diaminobenzidine (Sigma) and observed.

Statistical Assay

All data were obtained from no less than three independent reiterations and analyzed by SPSS 23.0 (SPSS, USA). Shapiro–Wilk test was used to check the normal distribution of all data. Pearson's correlation assay was implemented to reveal the correlation between two groups. Student's *t*-test was employed to examine the statistical differences between two groups, and ANOVA was administrated to compare the statistical differences among multiple groups. $P < 0.05$ was significant.

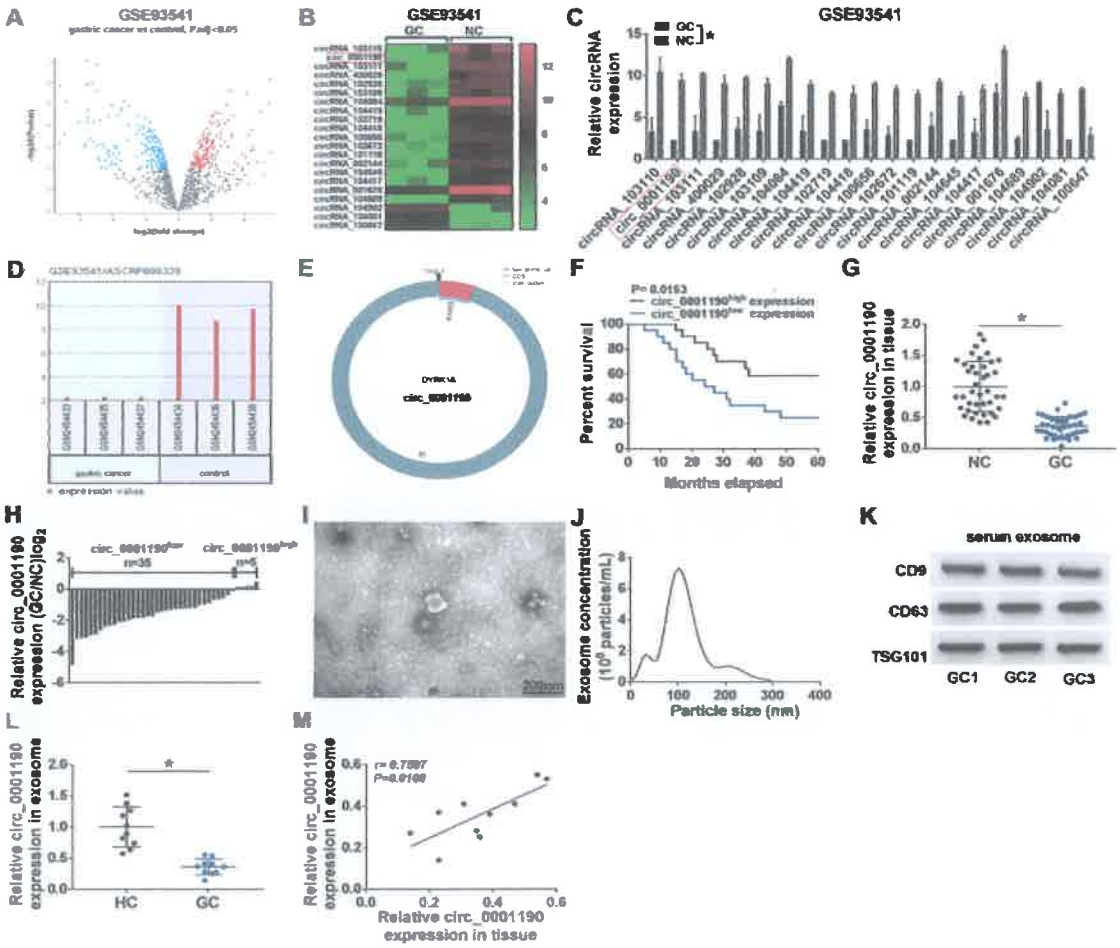

Fig. 1 Expression and validation of circ_0001190 in GC tissues and serum exosomes. **A** Volcano plot displayed circRNAs that altered prominently between GC tissues and matched normal tissues. **B** Cluster heat map presented the dissimilarly expressed circRNAs in paired human GC tissues and normal tissues. **C** The expression of circRNAs was assessed by qRT-PCR in paired human GC tissues and normal tissues. **D** The expression of circ_0001190 was examined by qRT-PCR. **E** The structure of circ_0001190. **F** The survival rate of GC patient. **G** and **H** The relative levels of circ_0001190 in GC tissues were detected by qRT-PCR. **I** Scanning of exosomes isolated from human plasma using electron microscopy. **J** NTA of plasma exosomes. **K** WB analysis of exosomal markers. **L** The relative levels of circ_0001190 in GC serum exosomes were examined by qRT-PCR. **M** Pearson's correlation analysis established that circ_0001190 in tissue was positive linked with circ_0001190 in exosome (R = 0.7597) in GC tissues. *$P < 0.05$

Results

Expression and Validation of circ_0001190 in GC Tissues and Serum Exosomes

Firstly, the GSE93541 database was used for the study. The volcano map showed that circRNAs that changed pointedly between GC and corresponding normal tissues (Fig. 1A). The cluster heat map shown in Fig. 1B indicated that circ_0001190 abundance was dramatically lesser in GC tissues. All the circRNA in this cluster heat map were differentially expressed (|log2FC|> 5 and $P<0.05$) between GC tissues and normal tissues. From the eligible circRNA (|log2FC|> 5 and $P<0.05$) in the GSE93541 database, we selected circ_0001190, which has a large difference in expression, to conduct a detailed study (Fig. 1C). Besides, in GSE93541 database, the expression of circ_0001190 was downregulated in GC tissues (Fig. 1D). Figure 1E showed that the circ_0001190 was a ring structure. Besides, among 40 GC patients, the group with low circ_0001190 expression had a relatively low survival rate compared with the group with high circ_0001190 (Fig. 1F). The results revealed that circ_0001190 was associated with the prognosis of GC. The circ_0001190 level was lower in GC tumor tissues ($n=40$) compared with that in para-cancerous tissues ($n=40$) (Fig. 1G). Then, the abundance of circ_0001190 in 40 paired GC tissues and para-cancerous tissues was detected. The circ_0001190 was downregulated in 35 GC tissues (Fig. 1H). Whereafter, we separated plasma exosomes from GC sufferers and normal subjects, and these exosomes were first analyzed by electron microscopy (Fig. 1I). The exosomes were about 100 nm in diameter, which was a typical size for exosomes (Fig. 1J). The exosomal markers CD9, CD63, and TSG101 were obviously measured in exosomes from all groups (Fig. 1K). The circ_0001190 level in exosome was abnormally lower in GC patient's plasma ($n=10$) compared with that in healthy person's plasma ($n=10$) (Fig. 1L). Pearson's correlation analysis unfolded that the circ_0001190 abundance in exosome was positive correlated with the circ_0001190 level in tissue (Fig. 1M). These results suggested that circ_0001190 was a downregulated circRNA derived from GC tissues and could be effectively delivered by exosomes into the circulation. Furthermore, a low abundance of circ_0001190 was linked with poor prognosis of GC, making it a possible marker of GC.

Expression and Validation of circ_0001190 in GC Cells and Cell Exosomes

We reconnoitered whether the abundance of circ_0001190 was unusual in GC cells and cell exosomes. The circ_0001190 level was evidently lower in GC cell lines (HGC27, AGS, MKN45, MKN47 and N87) compared with that in GES-1 cells (Fig. 2A). Among them, the level of circ_0001190 was lower in HGC27 and AGS cells, so they were used for subsequent experiments. Whereafter, we isolated GES-1, HGC27 and AGS cell lines exosomes and these exosomes were first examined by electron microscopy (Fig. 2B). The exosomes were about 100 nm in diameter, which was a typical size for exosomes (Fig. 2C).

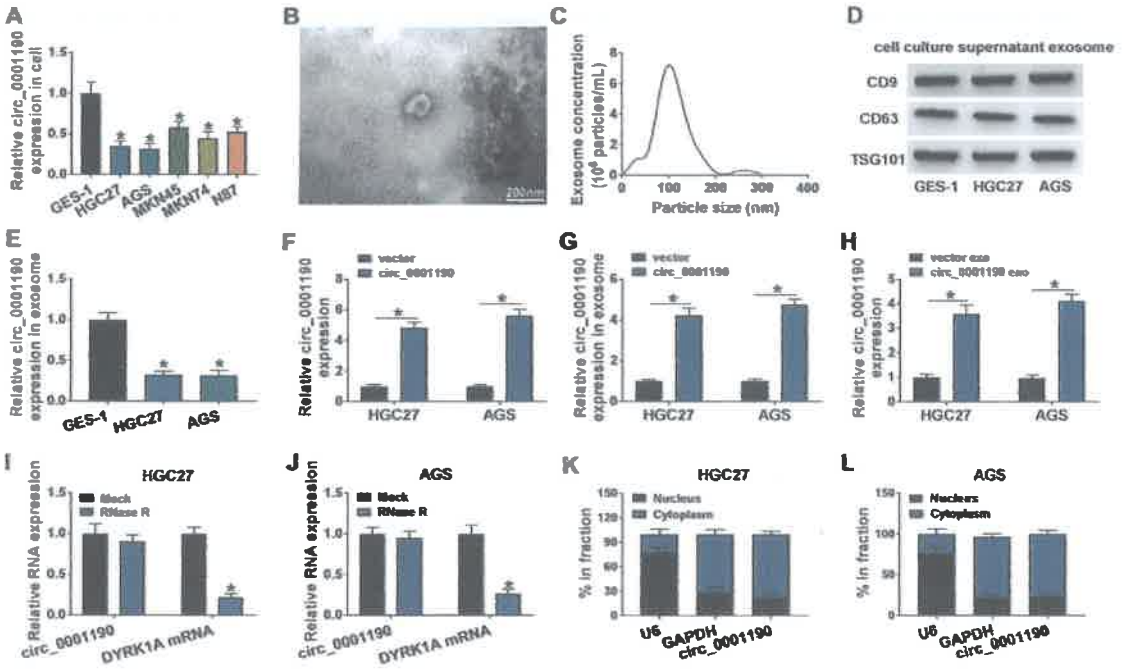

Fig. 2 Expression and validation of circ_0001190 in GC cells and cell exosomes. **A** The abundance of circ_0001190 in GC cells was quantified by qRT-PCR. **B** Scanning of exosomes isolated from GC cells using electron microscopy. **C** NTA of GC cells exosomes. **D** WB analysis of exosomal markers. **E** The relative content of circ_0001190 in GC cells exosome was distinguished by qRT-PCR. **F** and **G** The overexpression competence of circ_0001190 was measured by qRT-PCR. **H** The relative level of circ_0001190 was identified by qRT-PCR. **I** and **J** The relative levels of circ_0001190 and DYRK1A mRNA were assessed by qRT-PCR. **K** and **L** The relative level of circ_0001190 was exposed by qRT-PCR. $^*P < 0.05$

The exosomal markers CD9, CD63, and TSG101 were examined in exosomes from all groups (Fig. 2D). The qRT-PCR assay assessed that the circ_0001190 expression in exosome was dramatically lower in HGC27 and AGS cells versus that in GES-1 cells (Fig. 2E). In addition, circ_0001190 expression was memorably increased transfected with circ_0001190 compared to the vector group in HGC27 and AGS cells or cell exosomes (Fig. 2F and G). Meanwhile, the above overexpressed exosomes incubated with GC cells could increase the expression of circ_0001190 in GC cells (Fig. 2H). Preceding studies have shown, RNase R does not abridgment circular RNAs but only linear RNAs. As displayed in Fig. 2I and J, after the supplement of RNase R, the abundance of DYRK1A mRNA was significantly abridged, while the content of circ_0001190 was not changed. The consequence uncovered the cyclic structure of circ_0001190. Additionally, the content of circ_0001190 in cytoplasm was higher than that in nucleus (Fig. 2K and L). These outcomes exposed that circ_0001190 was down-regulation in GC cells, which could be delivered by exosomes into the circulation to take influence in GC. In addition, circ_0001190 structure was confirmed circular RNA.

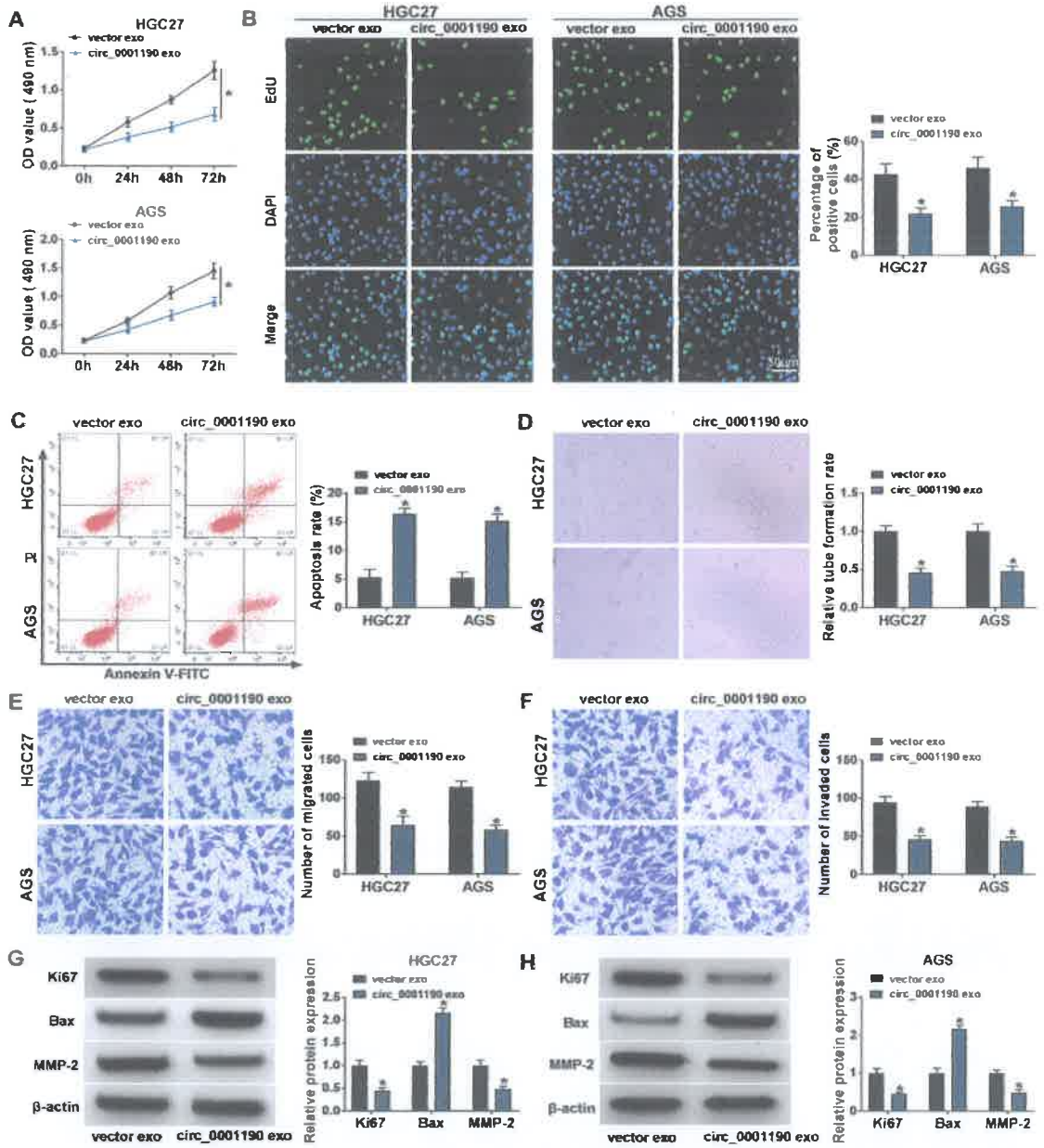

Fig. 3 Circ_0001190 subdued GC progression. **A** The CCK8 assay unfolded the cell vitality. **B** The EdU assay showed the cell proliferation. **C** The cell apoptosis was spotted by flow cytometry assay. **D** The tube formation assay detected the cell angiogenesis. **E** and **F** The transwell assay measured the cell migration and invasion. **G** and **H** The contents of Ki67, Bax, and MMP-2 were quantified by western blot. $^{*}P < 0.05$

Exosomal of circ_0001190 Overexpression Inhibited Cell Vitality, Cell Proliferation, Angiogenesis, Cell Migration and Invasion, Whereas Promoted Cell Apoptosis in GC Cells

Hence, to discover the character of circ_0001190 in GC, the functional assay was implemented. Figures 3A showed that circ_0001190 exo could remarkably decreased the cell vitality. In addition, the consequences of EdU assay discovered the circ_0001190 exo inhibited cell proliferation (Fig. 3B). In addition, the results

of flow cytometry assay uncovered the circ_0001190 exo promoted cell apoptosis (Fig. 3C). Moreover, the tube formation assay unfold that circ_0001190 exo suppressed the cell ability of angiogenesis (Fig. 3D). Meanwhile, transwell assay showed that circ_0001190 exo could restrain the cell migration and invasion in GC cells (Fig. 3E and F). Ki67, Bax and MMP-2 are associated with cell proliferation, apoptosis and cell migration, respectively. Here, we verified that circ_0001190 exo abridged the levels of Ki67 and MMP-2, but improved the content of Bax in GC cells (Fig. 3G and H). Our results indicated that exosomal of circ_0001190 overexpression inhibited cell vitality, cell proliferation, angiogenesis, cell migration and invasion, whereas endorsed cell apoptosis in GC cells.

MiR-586 Acted as the Target of circ_0001190 in GC Cells

Circinteractome and circbank predicted that the target miRNAs of circ_0001190 (Fig. 4A). The two databases predicted overlapping results for six miRNAs, comprising miR-576-5p, miR-586, miR-512-5p, miR-1827, miR-568, and miR-665. Among them, the expression of miR-586 had the most significant upregulated in GC tumor tissues ($n=3$) versus that in normal tissues ($n=3$) (Fig. 4B). Therefore,

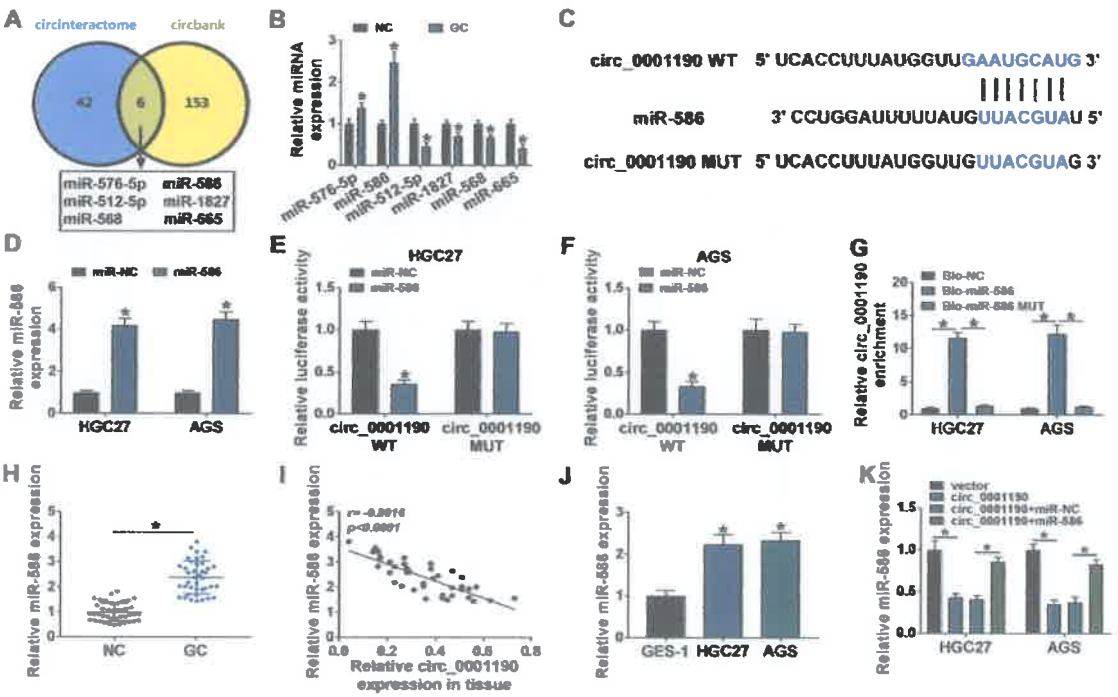

Fig. 4 Circ_0001190 sponged miR-586. **A** The targeted miRNAs of circ_0001190 were estimated by circinteractome and circbank. **B** The expressions of miRNAs were perceived by qRT-PCR. **C** The binding sites of miR-586 and circ_0001190. **D** The expression of miR-586 in GC cells was assessed by qRT-PCR. **E** and **F** Dual-luciferase reporter assay was utilized to confirm the association between circ_0001190 and miR-586. **G** RNA pull-down assay was exposed to substantiate the connection between circ_0001190 and miR-586. **H** The relative levels of miR-586 in GC tissues were measured by qRT-PCR. **I** Pearson's correlation analysis uncovered that circ_0001190 in tissue was negatively linked with miR-586 (R = -0.8016) in GC tissues. **J** and **K** The expression of miR-586 in GC cells was measured. *$P<0.05$

miR-586 was used for follow-up research. Figure 4C showed the binding sites of miR-586 and circ_0001190. Besides, the miR-586 expression was markedly increased by miR-586 mimic in GC cells (Fig. 4D). The luciferase activity was diminished in circ_0001190 WT and miR-586 mimic co-transfected in GC cells compared to circ_0001190 WT and miR-NC co-transfected, but there was no difference in circ_0001190 MUT and miR-586 mimic co-transfection groups (Fig. 4E and F). The RNA pull-down assay confirmed the straight mutuality between miR-586 and circ_0001190 in GC cells (Fig. 4G). In addition, the miR-586 was upregulated in GC tumor tissues ($n=40$) versus that in normal tissues ($n=40$) (Fig. 4H). Pearson's correlation analysis unfolded that the circ_0001190 content in tissue was negative correlated with the miR-586 expression in tissue (Fig. 4I). The miR-586 abundance was higher in GC cell lines (HGC27 and AGS) compared with that in GES-1 cells (Fig. 4J). Moreover, our data also suggested that the miR-586 expression was markedly declined by circ_0001190 overexpression, but augmented by miR-586 mimic (Fig. 4K).

MiR-586 Mimic Reversed circ_0001190 Exo Induced Inhibition in GC Cells

The miR-586 expression was markedly decreased by circ_0001190 exo, but increased by miR-586 mimic (Fig. 5A). Functionally, circ_0001190 exo inhibited the cell proliferation, but miR-586 mimic could diminish the impact in GC cells

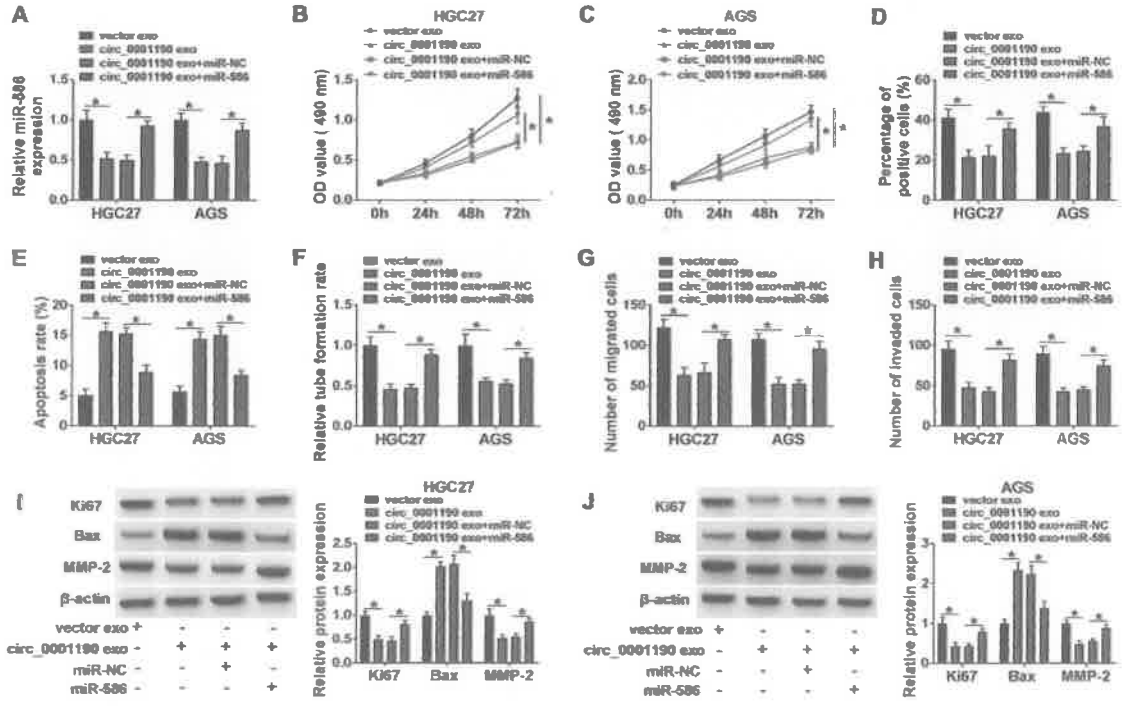

Fig. 5 Circ_0001190 subdued the advancement of GC by miR-586. **A** The miR-586 level was distinguished by qRT-PCR. **B** and **C** The cell vitality, **D** the cell proliferation, **E** the cell apoptosis, **F** the cell angiogenesis, **G** and **H** the cell migration and invasion, **I** and **J** the protein levels of Ki67, Bax, and MMP-2 were inspected by CCK8 assay, EdU assay, flow cytometry assay, tube formation assay, transwell assay, and western blot. $^*P<0.05$

(Fig. 5B–D). Besides, circ_0001190 exo promoted cell apoptosis, but miR-586 mimic could impair the impact in GC cells (Fig. 5E). Moreover, the circ_0001190 exo suppressed the cell ability of angiogenesis, whereas miR-586 mimic could lessen the impact in GC cells (Fig. 5F). Meanwhile, the circ_0001190 exo could restrain the cell migration and invasion, but miR-586 mimic could weaken the impact in GC cells (Fig. 5G and H). Besides, miR-586 mimic could inhibit the effect of circ_0001190 exo on the level of Ki67, Bax and MMP-2 in GC cells (Fig. 5I and J). Our consequences designated that circ_0001190 exo inhibited the growth of GC cells, whereas miR-586 mimic could lessen the impact.

MiR-586 Targeted SOSTDC1 in GC Cells

In GSE158662 database, only one eligible ($\log_2FC < -4$, $P < 0.05$) mRNA overlapped with TargetScan predicted miR-586 targeted mRNA, which was SOSTDC1 (Fig. 6A). Figure 6B shows the binding sites of miR-586 in SOSTDC1 3'UTR. The luciferase activity of SOSTDC1 3'UTR WT group was effectively reduced after miR-586 mimic transfection. Though, the luciferase activity of SOSTDC1 3'UTR MUT group was not altered by miR-586 (Fig. 6C and D). Our data also suggested that SOSTDC1 was downregulated in GC tumor tissues (n = 40) compared with that in normal tissues ($n = 40$) (Fig. 6E). In STAD based (http://ualcan.path.uab.edu/cgibin/TCGAExResultNew2.pl?genenam=

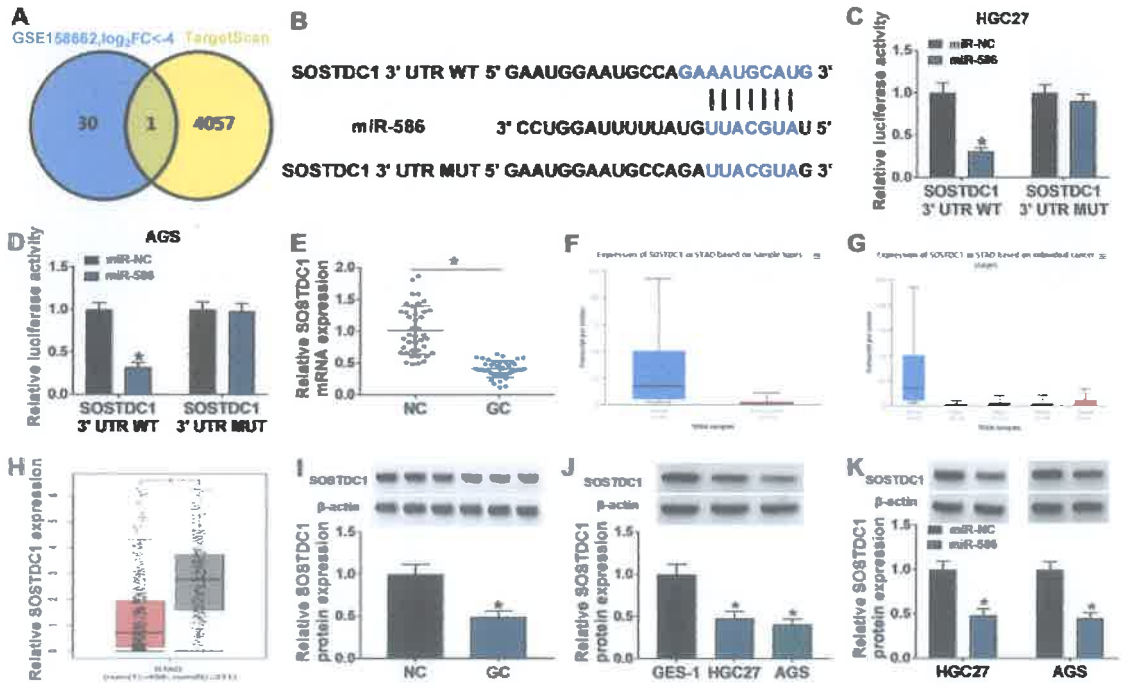

Fig. 6 MiR-586 targeted SOSTDC1 in GC cells. **A** The targeted gene of miR-586 was forecast by TargetScan. **B** The combinative sites between miR-586 and SOSTDC1. **C** and **D** Dual-luciferase reporter assay was enforced to check the link between miR-586 and SOSTDC1. **E** The SOSTDC1 content was detected by qRT-PCR. **F–H** The abundance of SOSTDC1. **I–K** The level of SOSTDC1 was detected by western blot. *$P < 0.05$

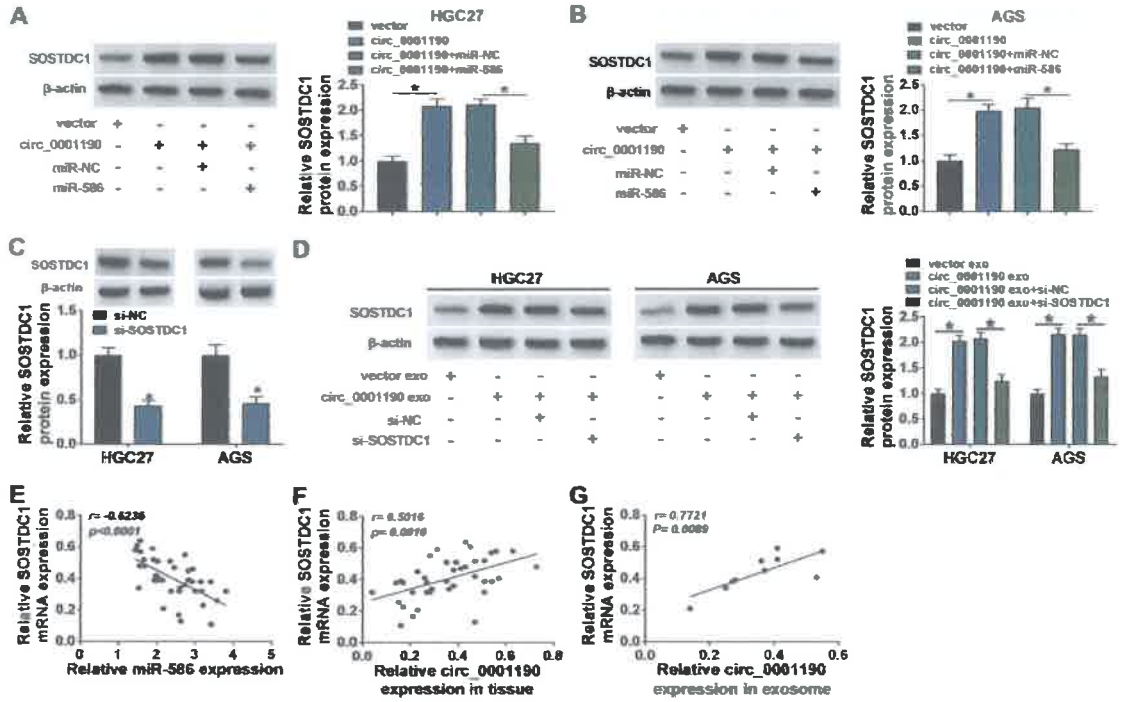

Fig. 7 Abundance of SOSTDC1 was adjusted by circ_0001190 and miR-586. **A–D** The expression of SOSTDC1 was distinguished by western blot. **E** Pearson's correlation analysis established that the level of SOSTDC1 was negatively linked with miR-586 (R = -0.6236) in GC tissues. **F** Pearson's correlation analysis exposed that circ_0001190 in tissue was positively associated with SOSTDC1 (R = 0.5016) in GC tissues. **G** Pearson's correlation analysis revealed that circ_0001190 in exosome was positive linked with SOSTDC1 (R = 0.7721) in GC tissues. $^{*}P < 0.05$

SOSTDC1&ctype=STAD), we found that the SOSTDC1 was downregulated in GC tumor tissues ($n = 415$) compared with that in normal tissues ($n = 34$) (Fig. 6F and G). In GEPIA based, we found that the SOSTDC1 was downregulated in GC tumor tissues ($n = 408$) compared with that in normal tissues ($n = 211$) (Fig. 6H). Figures 6I and J show that the protein level of SOSTDC1 was downregulated in GC tumor tissues ($n = 3$) and cells (HGC27 and AGS) compared with that in normal tissues ($n = 3$) and GES-1 cells. In addition, the SOSTDC1 content was diminished by transfected miR-586 mimic in GC cells (Fig. 6K). Furthermore, the level of SOSTDC1 was increased by transfected circ_0001190, but decreased by miR-586 mimic in GC cells (Fig. 7A and B). The SOSTDC1 protein level was markedly decreased by si-SOSTDC1 in GC cells (Fig. 7C). Meanwhile, the SOSTDC1 protein level was markedly increased by circ_0001190 exo, whereas decreased by si-SOSTDC1 in GC cells (Fig. 7D). Pearson's correlation analysis unfolded that the SOSTDC1 mRNA level in tissue was negative correlated with the miR-586 content in tissue (Fig. 7E). As the same way, the SOSTDC1 mRNA abundance in tissue was positive correlated with the circ_0001190 level in tissue (Fig. 7F). Besides, the SOSTDC1 mRNA expression in serum was positive correlated with the circ_0001190 expression in exosome (Fig. 7G). Collectively, these discoveries suggested that circ_0001190 promoted the expression of SOSTDC1 via miR-586.

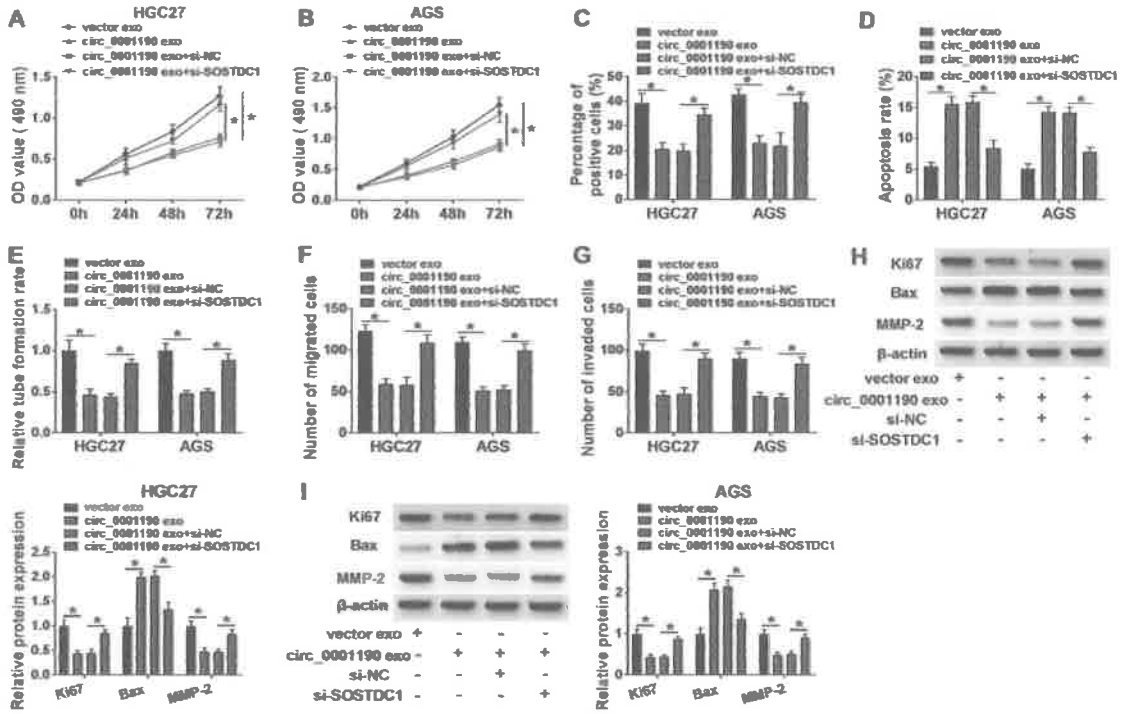

Fig. 8 Circ_0001190 adjusted the advancement of GC by regulating SOSTDC1. **A** and **B** The cell vitality, **C** the cell proliferation, **D** the cell apoptosis, **E** the cell angiogenesis, **F** and **G** the cell migration and invasion, **H** and **I** the protein contents of Ki67, Bax, and MMP-2 were examined by CCK8 assay, EdU assay, flow cytometry assay, tube formation assay, transwell assay, and western blot. $^*P < 0.05$

Silencing SOSTDC1 Reversed circ_0001190 Exo Induced Inhibition in GC Cells

Functionally, circ_0001190 exo inhibited cell proliferation, but SOSTDC1 deficiency could lessen the impact (Fig. 8A–C). Besides, circ_0001190 exo promoted cell apoptosis, but silencing SOSTDC1 could lessen the impact in GC cells (Fig. 8D). Moreover, the circ_0001190 exo reduced the cell ability of angiogenesis, whereas si-SOSTDC1 could lessen the impact in GC cells (Fig. 8E). Meanwhile, the circ_0001190 exo could restrain the cell migration and invasion, but SOSTDC1 deficiency could weaken the impact in GC cells (Fig. 8F and G). Besides, si-SOSTDC1 could inhibit the effect of circ_0001190 exo on the level of Ki67, Bax and MMP-2 in GC cells (Fig. 8H and I). Our results indicated that silencing SOSTDC1 could reverse circ_0001190 exo induced inhibition in GC cells growth.

Circ_0001190 Exo Restricted Tumor Growth In vivo

As shown in Fig. 9A–C, circ_0001190 exo treatment repressed tumor volume and weight. Then, the tumor tissues were examined. The circ_0001190 exo increased the level of circ_0001190, SOSTDC1, and Bax, but repressed the expression of miR-586, Ki67, and MMP-2 (Fig. 9D and E). The outcomes from IHC exposed that the abundance of Ki67 was lower, but SOSTDC1 was higher in the circ_0001190 exo

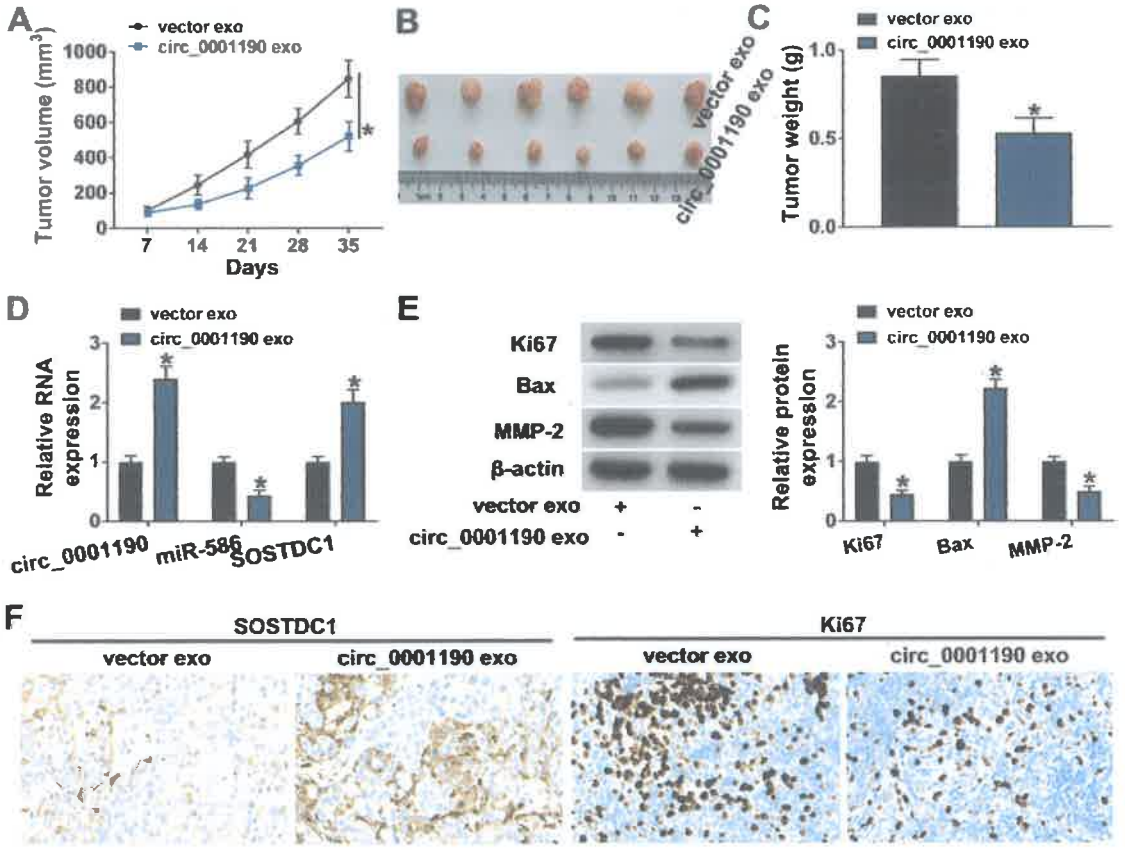

Fig. 9 Circ_0001190 restricted tumor growth. **A–C** The tumor volume and weight was assessed. **D** The abundances of circ_0001190, miR-586, and SOSTDC1 were discovered by qRT-PCR. **E** The contents of Ki67, Bax, and MMP-2 in these excised tumor tissues were detected by western blot. **F** IHC was applied to inspect the Ki67 and SOSTDC1 levels. $^{*}P < 0.05$

group compared with that in vector exo group (Fig. 9F). These consequences signposted that circ_0001190 exo repressed xenograft tumor growth.

Discussion

In current clinical practice, advanced GC was mainly treated by surgery (He et al. 2015). With the development of GC research, the emergence of many new targeted drugs has provided new ideas for the treatment (Shen et al. 2015; Zhang et al. 2015). Many molecular targeted agents have demonstrated significant antitumor activity in lots of molecular pathways, such as cell growth, cell cycle, angiogenesis, and invasion, providing molecular targets for cancer therapy (Huang et al. 2014; Lin et al. 2017). However, the functions of circ_0001190 in GC were still uncertain. Hence, our paper inspected the character of circ_0001190.

In our paper, we exposed that the circ_0001190 was downregulated in the GC, which is parallel to Liu et al. discoveries (Liu et al. 2020). Besides, circRanGAP1 regulated VEGFA abundance by binding miR-877-3p to elevate GC cell metastasis (Lu et al. 2020). Moreover, hsa_circ_0000745 was reduced in GC

and linked with GC cells differentiation (Huang et al. 2017). In addition, circDONSON facilitated GC growth, invasion, and apoptosis (Ding et al. 2019). Hsa_circ_001988 curbed GC development by interfering miR-197-3p (Sun et al. 2021). Herein, our consequences signposted that exosomal circ_0001190 overexpression inhibited cell vitality, cell proliferation, angiogenesis, cell migration and invasion, whereas promoted cell apoptosis in GC cells. Our results were similar to those of our predecessors. The circRNAs could competitively sponge for miRNAs, like circ_0004872 could target miR-224 in GC (Ma et al. 2020). In this study, exosomal circ_0001190 overexpression inhibited the progression of GC by sponging miR-586, which was parallel to former discoveries.

According to preceding information, miR-586 was relevant to the progress of glioma (Luo et al. 2020; Yang et al. 2015). In addition, miR-586 served as an oncogene via accelerating breast cancer (BC) growth and metastasis via ZEB1 (Zhang et al. 2021). Moreover, miR-586 might link with the risk of cervical cancer (Yu et al. 2020). Beyond that, miR-586 took part in adjusting the nephrotic syndrome development (Teng et al. 2015). In this paper, we discovered that miR-586 promoted the progress of GC by targeting SOSTDC1. This regulation mode was consistent with previous studies (Zhang et al. 2021). At present, many researches have proved that SOSTDC1 was associated with the development of BC, GC, and kidney cancer (Rawat and Gopisetty 2014; Gopal et al. 2013; Blish et al. 2008). Like, SOSTDC1 could contribute to cell invasion in colorectal cancer (Bartolome et al. 2020). In addition, BMP could antagonist SOSTDC1 to block GC development (Cui et al. 2019). Besides, SOSTDC1 served as a tumor-suppressive factor in GC and downregulation of it promoted tumor growth and boosted the formed of lung metastasis (Cui et al. 2019). In this paper, we got the same result as Cui et al. (Cui et al. 2019). In this research, the level of SOSTDC1 was downregulation in GC. Meanwhile, we witnessed that miR-586 reversed the increased effect of circ_0001190 on SOSTDC1 expression in GC cells. These outcomes additional sustained the control circuit of the circ_0001190/miR-586/SOSTDC1 in GC cells.

In brief, the paper determined that circ_0001190 and SOSTDC1 were downregulated and miR-586 was upregulated in GC. Furthermore, our study manifested that exosomal circ_0001190 overexpression inhibited cell vitality, cell proliferation, angiogenesis, cell migration and invasion, whereas promoted cell apoptosis in GC cells via miR-586/SOSTDC1 axis. There are still some limitations to the study, such as these data need further studied in clinical practice. Overall, this study provides clues to the regulatory mechanisms of GC and opens up new potential therapeutic avenues for future clinical targeted therapy.

Acknowledgements None

Funding None.

Declarations

Conflict of interest The authors declare that they have no conflicts of interest.

References

Ahn Y et al (2017) Multiple modes of Lrp4 function in modulation of Wnt/beta-catenin signaling during tooth development. Development 144:2824–2836

Allemani C et al (2018) Global surveillance of trends in cancer survival 2000–14 (CONCORD-3): analysis of individual records for 37 513 025 patients diagnosed with one of 18 cancers from 322 population-based registries in 71 countries. Lancet 391:1023–1075

Ambros V (2004) The functions of animal microRNAs. Nature 431:350–355

Bartolome RA et al (2020) SOSTDC1 promotes invasion and liver metastasis in colorectal cancer via interaction with ALCAM/CD166. Oncogene 39:6085–6098

Blish KR et al (2008) A human bone morphogenetic protein antagonist is down-regulated in renal cancer. Mol Biol Cell 19:457–464

Bray F et al (2018) Global cancer statistics 2018: GLOBOCAN estimates of incidence and mortality worldwide for 36 cancers in 185 countries. CA Cancer J Clin 68:394–424

Chen G et al (2018) SOSTDC1 inhibits bone metastasis in non-small cell lung cancer and may serve as a clinical therapeutic target. Int J Mol Med 42:3424–3436

Cui Y et al (2019) The BMP antagonist, SOSTDC1, restrains gastric cancer progression via inactivation of c-Jun signaling. Am J Cancer Res 9:2331–2348

Ding L et al (2019) Circular RNA circ-DONSON facilitates gastric cancer growth and invasion via NURF complex dependent activation of transcription factor SOX4. Mol Cancer 18:45

Garzon R, Marcucci G, Croce CM (2010) Targeting microRNAs in cancer: rationale, strategies and challenges. Nat Rev Drug Discov 9:775–789

Gopal G, Raja UM, Shirley S, Rajalekshmi KR, Rajkumar T (2013) SOSTDC1 down-regulation of expression involves CpG methylation and is a potential prognostic marker in gastric cancer. Cancer Genet 206:174–182

He W et al (2015) Surgical interventions for gastric cancer: a review of systematic reviews. Int J Clin Exp Med 8:13657–13669

Hou W, Zhang Y (2021) Circ_0025033 promotes the progression of ovarian cancer by activating the expression of LSM4 via targeting miR-184. Pathol Res Pract 217:153275

Huang J, Yang Y, Yang J, Li X (2014) Regenerating gene family member 4 promotes growth and migration of gastric cancer through protein kinase B pathway. Int J Clin Exp Med 7:3037–3044

Huang M, He YR, Liang LC, Huang Q, Zhu ZQ (2017) Circular RNA hsa_circ_0000745 may serve as a diagnostic marker for gastric cancer. World J Gastroenterol 23:6330–6338

Lee HS et al (2017) Molecular Testing for Gastrointestinal Cancer. J Pathol Transl Med 51:103–121

Li T et al (2018) Plasma circular RNA profiling of patients with gastric cancer and their droplet digital RT-PCR detection. J Mol Med (Berl) 96:85–96

Liang M et al (2019) Elevated levels of hsa_circ_006100 in gastric cancer promote cell growth and metastasis via miR-195/GPRC5A signalling. Cell Prolif 52:e12661

Lin Y et al (2017) Autocrine VEGF signaling promotes cell proliferation through a PLC-dependent pathway and modulates Apatinib treatment efficacy in gastric cancer. Oncotarget 8:11990–12002

Liu J, Li Z, Teng W, Ye X (2020) Identification of downregulated circRNAs from tissue and plasma of patients with gastric cancer and construction of a circRNA-miRNA-mRNA network. J Cell Biochem 121:4590–4600

Lu J et al (2020) Circular RNA circ-RanGAP1 regulates VEGFA expression by targeting miR-877-3p to facilitate gastric cancer invasion and metastasis. Cancer Lett 471:38–48

Luo Y et al (2020) Progress in the study of markers related to glioma prognosis. Eur Rev Med Pharmacol Sci 24:7690–7697

Ma C et al (2020) Circular RNA hsa_circ_0004872 inhibits gastric cancer progression via the miR-224/Smad4/ADAR1 successive regulatory circuit. Mol Cancer 19:157

Narhi K et al (2012) Sostdc1 defines the size and number of skin appendage placodes. Dev Biol 364:149–161

Qiu D et al (2018) RNF185 modulates JWA ubiquitination and promotes gastric cancer metastasis. Biochim Biophys Acta Mol Basis Dis 1864:1552–1561

Rawat A, Gopisetty G, Thangarajan R (2014) E4BP4 is a repressor of epigenetically regulated SOSTDC1 expression in breast cancer cells. Cell Oncol (dordr) 37:409–419

Shen Z et al (2015) The up-regulation of miR-300 in gastric cancer and its effects on cells malignancy. Int J Clin Exp Med 8:6773–6783

Shigetani Y et al (2008) Wise promotes coalescence of cells of neural crest and placode origins in the trigeminal region during head development. Dev Biol 319:346–358

Song Z, Wu Y, Yang J, Yang D, Fang X (2017) Progress in the treatment of advanced gastric cancer. Tumour Biol 39:1010428317714626

Sun Z et al (2015) Risk factors associated with splenic hilar lymph node metastasis in patients with advanced gastric cancer in northwest China. Int J Clin Exp Med 8:21358–21364

Sun D, Wang G, Xiao C, Xin Y (2021) Hsa_circ_001988 attenuates GC progression in vitro and in vivo via sponging miR-197-3p. J Cell Physiol 236:612–624

Teng J et al (2015) Differential microRNA expression in the serum of patients with nephrotic syndrome and clinical correlation analysis. Int J Clin Exp Pathol 8:7282–7286

Wang Q, Yu J (2018) MiR-129-5p suppresses gastric cancer cell invasion and proliferation by inhibiting COL1A1. Biochem Cell Biol 96:19–25

Wang GJ, Yu TY, Li YR, Liu YJ, Deng BB (2020a) Circ_0000190 suppresses gastric cancer progression potentially via inhibiting miR-1252/PAK3 pathway. Cancer Cell Int 20:351

Wang Z, Jiang Z, Zhou J, Liu Z (2020b) circRNA RNF111 regulates the growth, migration and invasion of gastric cancer cells by binding to miR27b3p. Int J Mol Med 46:1873–1885

Xie M et al (2020) Exosomal circSHKBP1 promotes gastric cancer progression via regulating the miR-582-3p/HUR/VEGF axis and suppressing HSP90 degradation. Mol Cancer 19:112

Yang L et al (2015) Downregulation of microRNA-586 Inhibits Proliferation, Invasion and Metastasis and Promotes Apoptosis in Human Osteosarcoma U2-OS Cell Line. Cytogenet Genome Res 146:268–278

Yu A et al (2020) Correlation Between Single Nucleotide Polymorphisms of an miRNA Binding Site in the 3'UTR of PTEN and Risk of Cervical Cancer Among the Han Chinese. Genet Test Mol Biomarkers 24:381–389

Zhang ZZ et al (2015) Analysis of plasma MicroRNAs to identifying early diagnostic molecule for gastric cancer. Int J Clin Exp Med 8:3700–3706

Zhang D et al (2021) LINC01189-miR-586-ZEB1 feedback loop regulates breast cancer progression through Wnt/beta-catenin signaling pathway. Mol Ther Nucleic Acids 25:455–467

Zheng P et al (2017) Exosomal transfer of tumor-associated macrophage-derived miR-21 confers cisplatin resistance in gastric cancer cells. J Exp Clin Cancer Res 36:53

Zhou Q et al (2017) SOSTDC1 inhibits follicular thyroid cancer cell proliferation, migration, and EMT via suppressing PI3K/Akt and MAPK/Erk signaling pathways. Mol Cell Biochem 435:87–95